

**CORTICAL MECHANISMS OF SENSORY MOTOR
ATTENUATION IN A SCI PARTICIPANT**

by

Teresa George

A thesis submitted to The Johns Hopkins University in conformity with the
requirements for the degree of Master of Science in Engineering.

Baltimore, Maryland

May, 2021

© 2021 Teresa George

All rights reserved

Abstract

Somatosensory attenuation (SMA) is a phenomenon where a self-generated touch feels weaker than an externally generated touch of the same intensity. The brain uses a forward model to predict the sensory consequences of our actions and in turn attenuates the afferent sensory feedback of our own movements. Even though SMA has been studied extensively, there is a lack of understanding of how the S1 multi-unit neurophysiology and the perception of SMA are correlated .

In this study, we record the perceptual and sensorimotor Multi-Unit Activity (MUA) of SMA in a chronically implanted SCI participant using a force comparison paradigm. We hypothesize that the perception of SMA will correlate with the S1 MUA. That is, when the two taps are of the same intensity, the S1 response for a self-generated tap will be lower than that of an externally generated tap and when the two taps are perceived to be the same at the Point of Subjective Equality (PSE), the S1 response will be the same for the two taps.

ABSTRACT

Additionally, we also perform a behavioral healthy controls comparison of SMA to study how SMA may vary between our SCI participant and healthy controls.

Contrary to our predictions, the perceptual and S1 neurophysiological amplification of self-generated force compared to an externally generated force was observed in our SCI participant when the two forces were of the same intensity. Importantly, we further found that there was a correlation between the perception of the force and the S1 MUA. That is, when the self-generated tap was perceived to be of a higher intensity compared to an externally generated tap of the same force intensity, the S1 MUA was higher for the self-generated tap compared to the externally generated tap. Similarly, when the two taps were perceived to be of the same intensity (at different absolute force intensities) at the PSE, the MUA in S1 for the two taps were similar.

The result of our study suggests that an amplification of self-generated stimulus is observed in our SCI participant and that the S1 MUA is related to the behavioral perception of force intensity.

Primary Readers and Advisors: Dr. Jeremy Brown and Dr. Gabriela Cantarero

Secondary Reader: Dr. Vikram Chib

Acknowledgments

I would like to give my sincere gratitude to my primary advisors Dr. Jeremy Brown and Dr. Gabriela Cantarero for introducing me to the world of scientific research and for their constant support and guidance throughout the completion of this project. I would like to thank Dr. Vikram Chib for reading my thesis and giving me valuable suggestions. I would like to especially thank Dr. Agostina Casamento-Moran and Mohit Singhala for all their contributions towards this project and for helping me in every way possible in completing my thesis. I wish to also extend my thanks to Dr. Robert Nickl for teaching me neural data analysis and for always being available to answer all my questions. Special thanks to Dr. David McMullen for all his invaluable insights and suggestions towards this project.

I would also like to extend my gratitude towards all the other members of the BiCNS team for all the help throughout my research journey here and our SCI research participant for being very cooperative and patient and for making all the experimental sessions a really fun experience.

ACKNOWLEDGMENTS

Finally, I would like to thank my parents and my brother for their love, encouragement and support throughout this journey, my roommates Mallika and Debolina for always being there for me and all my other friends in Baltimore who have made these two years wonderful and have made Baltimore a home away from home.

Dedication

To my mom and dad for always loving me, believing in me and giving me all the countless opportunities I could have ever asked for.

Contents

Abstract	ii
Acknowledgments	iv
List of Figures	x
1 Introduction	1
2 Materials and Methodology	5
2.1 Experimental Paradigm	5
2.2 Participants	7
2.3 Data Recordings and preprocessing	9
2.3.1 Force Recordings	9
2.3.2 MUA data acquisition and preprocessing	11
2.4 Data Analysis	13
2.4.1 Characterizing Contralateral S1 Responses to Movement Preparation	13

CONTENTS

2.4.2	Characterizing Contralateral S1 Responses to Sensory Taps	14
2.4.3	Quantifying Somatosensory Attenuation	16
2.5	Statistical Analysis	17
2.5.1	Calculating difference in MOR across condition	17
2.5.2	Calculating difference in the neural firing rate between Baseline 1(B1) and Baseline (B2)	18
3	Results	19
3.1	Comparison of behavioral perception of SMA in SCI participant and healthy controls	19
3.2	Matched-force comparison: Comparison of contralateral S1 MUA in response to 2N active reference tap and 2N no movement reference tap	20
3.3	Matched-perception comparison: Comparison of contralateral S1 MUA for self-generated tap of 2N and externally generated tap at the PSE	24
3.4	Change in the MOR for matched-force and matched-perception: Comparison between Δ MOR for matched-force and matched-perception	25
3.5	Average MOR response for all no-movement comparison force intensities	28

CONTENTS

3.6 Preparatory neural activity: Comparison between average neural firing rate in baseline 1(B1) and baseline 2 (B2)	29
4 Observation and Conclusion	32
4.1 Observation	32
4.2 Limitations and Next Steps	37
4.3 Conclusion	38
Vita	49

List of Figures

- 2.1 **Hand Alignment and Experimental Paradigm:** (A) Image shows the hand positioning for the bimanual paradigm with both hands aligned closely together. The custom-built device consisted of a force sensor, (LC61SP-2KG, weight capacity, 2kgf) that was used to measure the force applied by the participant. The taps are delivered to the pulp of the participant’s index finger using a 3D printed ABS probe (with a circular contact area of 25 mm^2) that is attached to an electric DC motor (Maxon RE 50). (B) Image shows the active movement condition of the experimental paradigm. In the active movement condition, participants actively tapped a force sensor with their left wrist that generated a reference tap on their right index finger, which was then followed by a second externally generated comparison tap. (C) Image shows the no movement condition of the experimental paradigm. In the no movement condition, participants remained relaxed and received a reference tap externally which is then followed by a second externally generated comparison tap. In both conditions, after receiving both taps, the participants indicated which of the two taps felt to be of a stronger intensity. 8
- 2.2 **MEA implantation location:** 6 MEAs were implanted in the left and right hemisphere: three 96-channel arrays in bilateral motor cortex (2 (Pedestal A and Pedestal B) in left hemisphere and 1(Pedestal C) in right hemisphere) and three 32-channel arrays in bilateral sensory cortex (2 (Pedestal A and Pedestal B) in left hemisphere and 1(Pedestal C) in right hemisphere). MEAs are shown in white, and the yellow dotted line represents the central sulcus (reprinted from Tessy Thomas et. al, 2020). 10

LIST OF FIGURES

- 2.3 **Neural activity response across time:** The figure shows the neural activity response across time for a single experimental trial. The four black dashed lines represent the four analog event signals used to align the neural data for offline analysis. The first analog signal is the auditory instructional cue, that instructs the participant about the type of trial. The second analog signal is auditory Go/No Go cue. The third analog signal represents the onset of the reference tap (tap 1), the fourth auditory cue represents the onset of the comparison tap (tap 2). We considered four 500ms neural activity windows with respect to each of these four event signals (Baseline 1(BL1), Baseline 2(BL2), Response 1(R1) and Response 2(R2)). Note: R1 could either be an active movement reference tap or a no movement reference tap while R2 is always a comparison tap. 12
- 3.1 **Behavioral response for SMA in healthy participants (n=3) and SCI participant:** A) The psychometric curve for the SCI participant. The psychometric curve in the active movement condition shifts towards the right indicating a perceptual amplification of self-generated tap when compared to an externally generated tap of the same force intensity of 2N in SCI participant. The x axis denotes the comparison force values and the y-axis denotes the probability that the comparison force is higher than the reference force. Green line represents the no-movement condition, and the red line represents the active movement condition. B) Psychometric curve for healthy participants. The psychometric curve in the active movement condition shifts towards the left indicating a perceptual attenuation of self-generated tap when compared to an externally generated tap of the same force intensity of 2N in healthy participants. The x axis denotes the comparison force values and the y-axis denotes the probability that the comparison force is higher than the reference force. Green line represents the no-movement condition, and the red line represents the active movement condition. C) Bar graph showing the change in PSE between the active movement and no movement condition. SCI participant PSE for active movement condition is 2.11N and the PSE for no movement condition is 1.99N (SMA=+0.12N (yellow)). For healthy participants, average PSE for active movement condition is 1.747 and PSE for no movement condition is 1.864 (SMA=-0.117(light purple)). y-axis denotes the change in PSE. 21

LIST OF FIGURES

- 3.2 Matched-force comparison- S1 response for active movement reference tap and no movement reference tap at force intensity of 2N:** A) Represents the sensory MEAs in the participants contralateral hemisphere (top from Pedestal A and bottom from Pedestal B). Channels that are highlighted in blue represent a significant difference in the magnitude of response (MOR) between the active movement and no movement reference tap of 2N. An example PETH for the channels is marked by a pink circle and expanded upon in 3.2B. B) Example PETH plots of two channels that show significant difference in the MOR in Pedestal A (top) and B (bottom) show the neural response in S1 to the active movement reference tap at 2N (in red) and the no movement reference tap at 2N (in green). The dashed black line represents the time of the tap stimulus onset (reference tap). The x-axis denotes the time (in s) and y-axis denotes the firing rate in spikes/s. C) The bar graph shows the average MOR (mean \pm SEM) for the active movement reference tap of 2N (red) and the no movement reference tap of 2N (green). The average MORs for the active movement was significantly higher than the no movement condition for both pedestal A and B (** $p < 0.001$). y-axis denotes the average MOR in spikes/s. 23

LIST OF FIGURES

- 3.3 Matched-perception comparison: S1 multi-unit neural response for 2N active reference tap and comparison tap at PSE (2.1 N comparison tap):** A) Represents the sensory MEAs for Pedestal A (top) and B (bottom) sensory channels of the contralateral hemisphere. No channels in Ped A showed a significant difference in the MOR between the two matched-perception conditions and only 1 channel in pedestal B (highlighted by blue) showed a significant difference in the MOR between the two conditions ($p < 0.05$). B) Example PETH plots of channels highlighted by pink circle in figure 3.3A. The peak S1 response to the two matched-perception forces appear similar. The dashed black line represents the time of the tap stimulus onset (reference tap/ comparison tap). The x-axis denotes the time (in s) and y-axis denotes the firing rate in spikes/s. C) The bar graph shows the average MOR (mean \pm SEM) for the active movement reference tap (red) at 2N and the 2.1N PSE comparison tap (green). There was no significant difference in Pedestal A between the active movement reference tap of 2N (red) and the PSE comparison tap at 2.1N (green), ($p = 0.6866$), however, there was in Pedestal B, with 2N reference tap average MOR (red) showing a significant increase compared to the 2.1N PSE (green) ($p = 0.03$). y-axis denotes the average MOR in spikes/s. (* $p < 0.05$ denoting significantly different, n.s denotes not significantly different) 26
- 3.4 Change in average MOR(Δ) between the matched-force and the matched-perception conditions:** A) Shows the change in average MOR between the matched-force condition (2N active ref. Vs 2N no movement ref.) and the matched-perception condition (2N active ref. Vs 2.1N (PSE) comparison) in pedestal A. The change in MOR was significantly greater in the matched-force condition as compared to matched-perception condition (** $p < 0.001$). B) Shows the change in average MOR between the matched-force condition (2N active ref. Vs 2N no movement ref.) and the matched-perception condition (2N active ref. Vs 2.1N (PSE) comparison) in pedestal B. Similarly, there was a significantly greater change in MOR for the matched-force as compared to matched-perception condition. (** $p < 0.001$). y-axis denotes the average MOR in spikes/s. 27

LIST OF FIGURES

- 3.5 Average contralateral S1 MOR response for all comparison forces:** A) Bar graph represents the Average MOR (+/-SEM) for all the different comparison force intensities (1N, 1.5N, 1.75N, 1.9N, 2N, 2.1N, 2.25N, 2.5N, 3N) in pedestal A (* $p < 0.05$, ** $p < 0.01$, *** $p < 0.001$). y-axis denotes the average MOR in spikes/s.
B) Bar graph represents the Average MOR+/-SEM for all the different comparison force intensities (1N, 1.5N, 1.75N, 1.9N, 2N, 2.1N, 2.25N, 2.5N, 3N) in pedestal B (* $p < 0.05$, ** $p < 0.01$, *** $p < 0.001$). y-axis denotes the average MOR in spikes/s. 30
- 3.6 Comparison of the average firing rate between B1 and B2:** Bar graph represents the average firing rate (+/-SEM) in B1 (purple) and the average firing rate (+/-SEM) in B2 (beige) for pedestal A and B combined. The y-axis denotes the average firing rate in spikes/s. (n.s (not significant)) 31

Chapter 1

Introduction

Somatosensory attenuation (SMA) is a phenomenon wherein a self-generated force feels weaker than an externally generated force of the same intensity¹⁻⁵. Similar mechanisms also occur in other sensory domains such as the auditory and visual domain where we suppress the auditory response of our own self-produced speech (as compared to passively listening to the same speech)^{6;7} and suppress images on our retina as we saccade to maintain a stable image of our environment^{8;9}. SMA helps us pay greater attention to external stimuli from the environment by reducing the cognitive consequences of our own actions².

In the somatosensory domain, several behavioral studies in humans have shown that the perception of self-produced forces are perceived as less intense than their true force^{1;3;10}. For example, when an externally generated tap on

CHAPTER 1. INTRODUCTION

the left finger is synchronously timed with the execution of an input tap from the right finger (simulating contact between the fingers), the perception of force in the left finger is attenuated relative to an identical externally generated tap without the corresponding input tap.

Several factors affect the magnitude of sensorimotor attenuation such as the distance and timing of sensory feedback and experience^{3;11;12}. When a self-generated force is applied from one hand to the other, if the distance between the hand that moves and the hand that receives the afferent feedback is 25 cm or more somatosensory attenuation is abolished. Similarly, if the timing of the user's movements and the sensory consequences of the tap are delayed and are not predictable^{4;12}, somatosensory attenuation is abolished. However, if the sensory consequences of a movement are altered in a predictable way, with sufficient repetition, SMA re-emerges¹² as the new timing relationship is learned. This suggests that agency (i.e., the subjective ability of controlling one's own actions), which can be learned through experience, is a critical component of SMA.

Additionally, some disorders of the central nervous system have also been shown to alter SMA. Patients with multiple sclerosis and Parkinson's Disease lack SMA for self-generated forces¹³⁻¹⁵. Likewise, patients with psychological

CHAPTER 1. INTRODUCTION

disorders such as Schizophrenia have an absent somatosensory attenuation and this loss of SMA is thought to contribute to the delusions of control in these patients¹⁶.

It is theorized that the neural mechanisms of SMA arise from the internal forward model that the brain uses for planning and executing a movement^{2;17-23}. Every time we make a movement, a copy of the motor command generated in the primary motor cortex (M1), called an efference copy, is sent to other cortical areas such as the cerebellum and the primary somatosensory cortex (S1). With this information the brain can predict the sensory consequences of our own actions and attenuate the afferent sensory feedback of our own movements, thereby increasing the saliency of external signals.

Many studies in humans have shown that there is a reduction in the somatosensory evoked responses in S1 preceding and following the actual active movement^{16;24;25}. For example, the amplitude of the somatosensory evoked potentials (SEPs) and somatosensory-evoked magnetic fields are reduced before the onset of movement^{26;27}. Similarly, blood oxygen level-dependent (BOLD) response in S1 is reduced when the tactile stimuli are caused by one's own movement compared with when they are externally triggered^{5;11;28}. In one animal study with non-human primates (NHP), intracortical microstimulation

CHAPTER 1. INTRODUCTION

(ICMS) of M1 prior to movement onset has been shown to reduce somatosensory evoked neural activity in S1²⁹.

Though NHP data suggest that ICMS of M1 can suppress S1 activity evoked by tactile feedback, no studies in NHPs nor humans have studied the role of S1 in SMA at a multi-unit neural level. Here we aimed to understand the S1 neurophysiological correlate of SMA and how it relates with perceptual behavior. We hypothesized that S1 MUA for a self-generated tap as compared to an externally generated tap of the same force would be associated with a reduction in S1 firing rate that would correlate with a reduced percept of somatosensation.

To test this hypothesis, we simultaneously recorded perceptual and S1 multi-unit neural activity (MUA) during a bimanual, force comparison, self-touch paradigm to compare self-generated and externally generated somatosensory feedback. This was done in a chronically implanted human spinal cord injury participant with intact sensation and residual motor abilities. Additionally, we compared behaviorally how perceptual measures of SMA may vary between our spinal cord injury participant and a group of healthy controls.

Chapter 2

Materials and Methodology

2.1 Experimental Paradigm

Using a custom-built device that simulates bimanual self-touch, we used a two-alternative force choice (2AFC) task with the method of constant stimuli to quantify somatosensory attenuation. Concurrently, we recorded from micro-electrode arrays (MEAs) in bilateral sensorimotor areas in a chronically implanted spinal cord injury participant. In this paradigm, the participant kept his right index finger at rest (palm facing inward toward his left hand) and the back side of his left hand was resting next to the force sensor - in this way both hands were closely aligned with the right hand resting in front of the left hand (Fig 2.1). The participant received two taps 1000ms apart from each other on the tip of his right index finger and was asked to report which tap felt stronger.

CHAPTER 2. MATERIALS AND METHODOLOGY

The first tap (i.e. reference tap) was generated either by the participant with a wrist-extension tap or externally generated by a motor, in both cases the applied force was at a fixed value of 2N. The second tap (i.e. comparison tap) was always externally generated by a motor and consisted of a range of force values: 1N, 1.5N, 1.75N, 1.9N, 2N, 2.1N, 2.25, 2.5N and 3N. In this way, the paradigm included two conditions: an active movement and no-movement condition. Before each trial, the participant was informed whether the subsequent trial would be an ‘active movement’ or ‘no movement’ condition. In the ‘active movement’ condition, the participant was instructed to extend his left wrist to generate a 2N tap against the force sensor in response to an auditory “Go” cue. The active tap on the force sensor triggered a 2N reference tap on his right index finger which was then followed by an externally generated comparison tap. In the ‘no movement’ condition, participant was instructed to relax his left wrist in response to a “No Go” cue and received an externally generated reference tap of 2N, followed by an external comparison tap on the right index finger. For both the active and no movement condition, the participant was asked to report which tap (reference or comparison) felt stronger after each trial. There were a total of 360 trials completed across both conditions such that each reference and comparison tap combination was repeated 20 times.

Note that the hand positioning and paradigm was specifically selected to

CHAPTER 2. MATERIALS AND METHODOLOGY

maximize the residual motor function of the SCI participant's left wrist in addition to his clinically normal sensory perception in his hands. To compare whether SMA may be altered in our SCI participant, we additionally recruited a group of healthy controls that performed the identical 2AFC paradigm as described above. In this group only perceptual measures were collected.

Prior to the main experiment, all participants were trained to consistently generate a 2N tap against the force sensor by extending their wrist. During the experiment, participants' performance was monitored continuously by the experimenter and were provided with verbal feedback when they deviated by more than ± 1 N from the 2N target.

2.2 Participants

A 50-year old male with C5-C6 ASIA B tetraplegia (32 years post injury; right hand dominant) was implanted bilaterally with six cortical microelectrode arrays (MEAs) in the his sensorimotor hand representations (NeuroPort; Blackrock Microsystems, Salt Lake City, UT): four in the left hemisphere (2 in M1, 2 in S1-Pedestal A and Pedestal B), and two in the right (1 each in M1 and S1- Pedestal C) (Fig 2.2). Each motor array consisted of 96, 4X4mm channels (platinum tip) and each sensory array consisted of 32, 4X2.4mm chan-

CHAPTER 2. MATERIALS AND METHODOLOGY

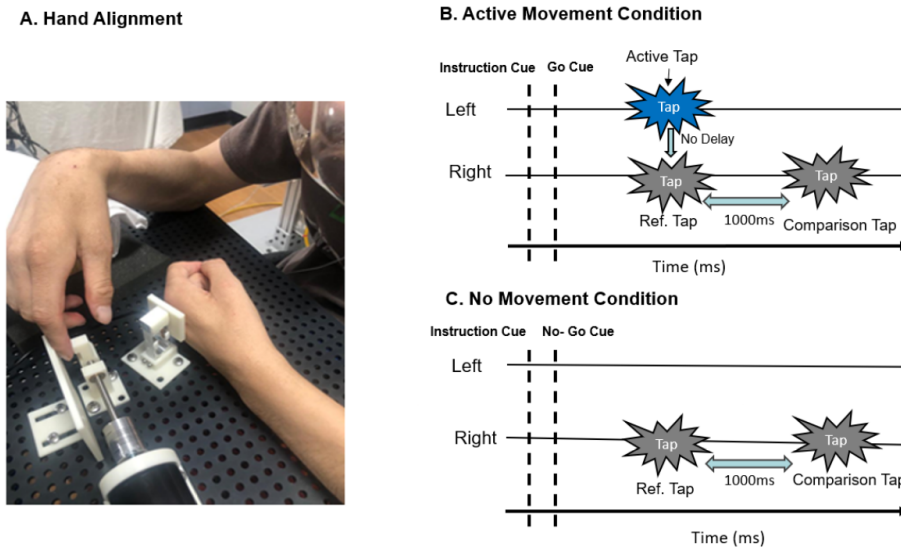


Figure 2.1: Hand Alignment and Experimental Paradigm: (A) Image shows the hand positioning for the bimanual paradigm with both hands aligned closely together. The custom-built device consisted of a force sensor, (LC61SP-2KG, weight capacity, 2kgf) that was used to measure the force applied by the participant. The taps are delivered to the pulp of the participant's index finger using a 3D printed ABS probe (with a circular contact area of 25 mm^2) that is attached to an electric DC motor (Maxon RE 50). (B) Image shows the active movement condition of the experimental paradigm. In the active movement condition, participants actively tapped a force sensor with their left wrist that generated a reference tap on their right index finger, which was then followed by a second externally generated comparison tap. (C) Image shows the no movement condition of the experimental paradigm. In the no movement condition, participants remained relaxed and received a reference tap externally which is then followed by a second externally generated comparison tap. In both conditions, after receiving both taps, the participants indicated which of the two taps felt to be of a stronger intensity.

CHAPTER 2. MATERIALS AND METHODOLOGY

nels (sputtered iridium oxide film-tipped). Implantation placement of the arrays was performed using a combination of pre-operative 7T structural and functional MRI (fMRI) during attempted/executed arm and hand movements to identify M1 locations and a novel intraoperative online functional mapping technique with high-density electrocorticography (ECoG) to localize S1 fingertip representations (see McMullen et al. 2020 for more details on the implantation procedure). Clinical assessments showed that the participant had intact sensation to touch stimulation on all fingers. As a control, we also recruited three healthy participants (Average Age 26.6 +/- 3.05), 2 Female) to complete the behavioral portion of the experiments. This study was conducted under an Investigational Device Exemption (IDE) by the FDA (G170010) and approved by the Johns Hopkins School of Medicine and NIWC Pacific Institutional Review Boards (IRBs).

2.3 Data Recordings and preprocessing

2.3.1 Force Recordings

The force data from the force sensor was recorded real-time at a sampling rate of 1kHz on Quanser Q8-USB DAQ and on Neuroport Neural Signal Processors (Blackrock Microsystems) using analog channels.

CHAPTER 2. MATERIALS AND METHODOLOGY

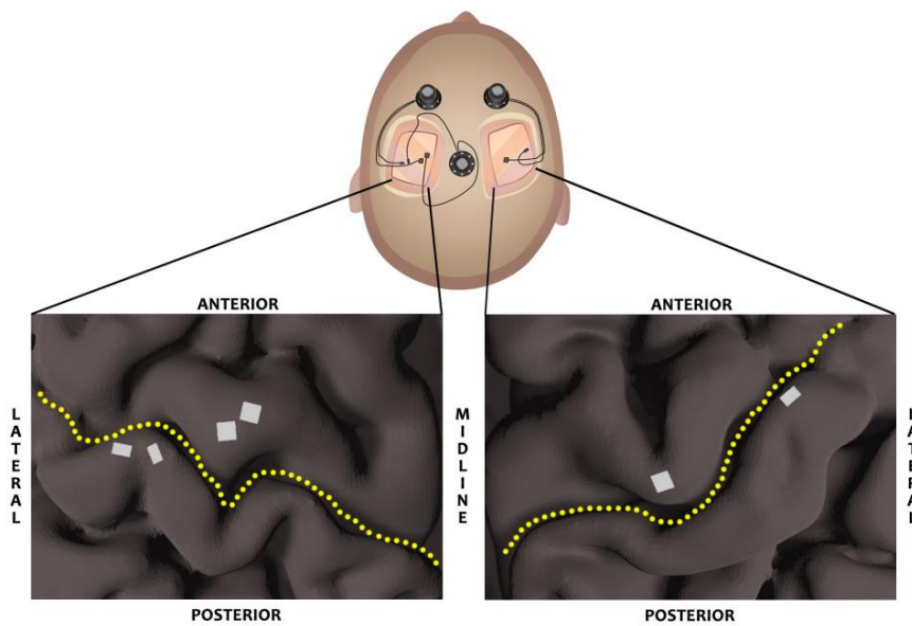


Figure 2.2: **MEA implantation location:** 6 MEAs were implanted in the left and right hemisphere: three 96-channel arrays in bilateral motor cortex (2 (Pedestal A and Pedestal B) in left hemisphere and 1(Pedestal C) in right hemisphere) and three 32-channel arrays in bilateral sensory cortex (2 (Pedestal A and Pedestal B) in left hemisphere and 1(Pedestal C) in right hemisphere). MEAs are shown in white, and the yellow dotted line represents the central sulcus (reprinted from Tessy Thomas et. al, 2020).

2.3.2 MUA data acquisition and preprocessing

Multiunit activity (MUA) was recorded at a sampling rate of 30kHz using Neuroport Neural Signal Processors (Blackrock Microsystems). The recordings for each channel were auto-thresholded at -3.5 times the root mean square voltage (RMS) of resting state activity. A high pass filter of 250 Hz was used for spike processing. To align the neural and behavioral data and facilitate offline analysis, we recorded four 4 analog events at 1kHz sampling rate on the Neuroport Neural Signal Processors: (1) auditory cue instructing the participant about the type of trial (instruction cue), (2) auditory cue instructing “go/no go” cue (Go/No-Go Cue), (3) reference tap (i.e. first tap provided to participant’s index finger), (4) comparison tap (i.e. the second tap provided to participant’s index finger) (Fig 2.3).

Prior to analysis, spiking times were binned into peri-stimulus time histograms (PSTHs) at a resolution of 0.5 ms. All neural activity measures are based on raw PSTHs and only smoothed (using Gaussian kernels of width 300ms) for visualization purposes. Experimental software and analyses were coded in MATLAB (MathWorks, Natick, MA). Channels whose activity was directly attributable to jaw muscle artifacts were excluded from further analysis.

CHAPTER 2. MATERIALS AND METHODOLOGY

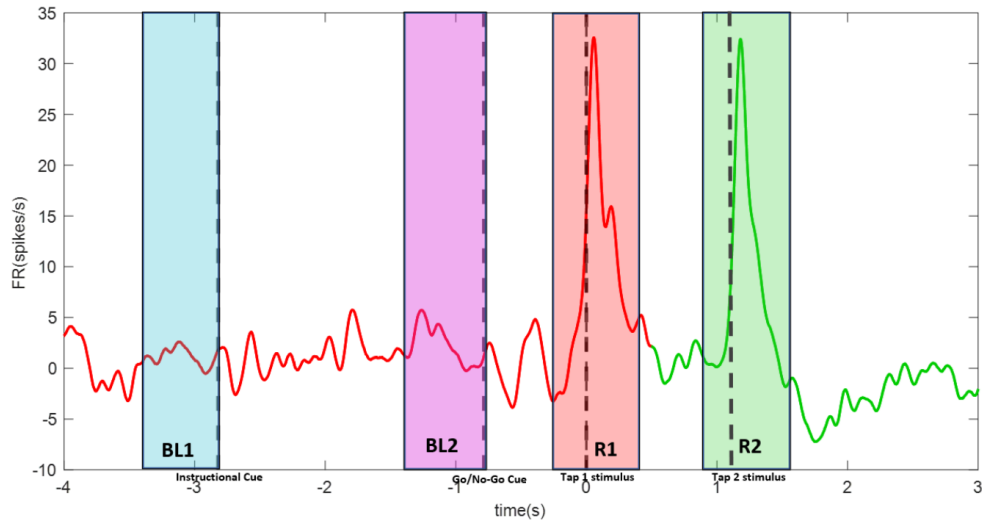


Figure 2.3: Neural activity response across time: The figure shows the neural activity response across time for a single experimental trial. The four black dashed lines represent the four analog event signals used to align the neural data for offline analysis. The first analog signal is the auditory instructional cue, that instructs the participant about the type of trial. The second analog signal is auditory Go/No Go cue. The third analog signal represents the onset of the reference tap (tap 1), the fourth auditory cue represents the onset of the comparison tap (tap 2). We considered four 500ms neural activity windows with respect to each of these four event signals (Baseline 1(BL1), Baseline 2(BL2), Response 1(R1) and Response 2(R2)). Note: R1 could either be an active movement reference tap or a no movement reference tap while R2 is always a comparison tap.

This was done by eliminating all trials in all microelectrode array channels that had a neural firing rate above 150 spikes/s for a duration of 150ms or more in any of the baseline or response windows that were considered in our neural data analysis. (Note we decided to use this metric as our threshold to determine trials attributed to jaw muscle artifacts by visually inspecting PETH plots for various trials).

2.4 Data Analysis

2.4.1 Characterizing Contralateral S1 Responses to Movement Preparation

Neural activity from all contralateral sensory channels (i.e., left hemisphere (Pedestal A and B)) were calculated as the average firing rate per trial over a fixed 500ms time window. We identified two regions of interest to examine preparatory activity: Baseline 1 (B1) and Baseline 2 (B2). B1 represented the true baseline neural activity (i.e., time period in which the participant was naive to the type of trial that would follow) and was calculated as the average firing rate from -500ms to 0ms relative to the instructional cue. B2 represented the preparatory baseline (i.e., time period in which the participant was anticipating either an active or no movement trial) and was calculated as -500ms to 0ms relative to the Go/No-Go cue. Changes in B1 and B2 for the active movement condition were used to assess whether there were any shift in the baseline firing rate prior to the instructional cue as compared to prior to movement onset.

2.4.2 Characterizing Contralateral S1 Responses to Sensory Taps

Response activity to the reference tap (R1), from all contralateral sensory channels, was calculated as the average firing rate from -200ms to 300ms relative to the first tap; responsive activity to the comparison tap (R2) was calculated as the average firing rate from -200ms to 300ms relative to the second tap. Presence of a significant response to the tap stimuli was detected by comparing the R1 firing rate to the B1 firing rate using a two-sided statistical test. If the channels exhibited a normal distribution of firing rates, we used a paired sample t-test, otherwise we used a two-sided Wilcoxon signed-rank test. We control for multiple comparisons across channels using the false discovery rate (FDR) [Benjamini & Hochberg, 1995]. Channels that had a significant change in R1 as compared to B1 were defined as ‘active channels’. For all ‘active channels’ (i.e., channels that showed a significant change in activity to the response tap), we calculated a Magnitude of Response (MOR) for each tap stimuli (reference and comparison) separately. This consisted of calculating the average response window activity from 0ms to 250ms relative to the tap stimulus and subtracting a shortened B1 activity (from -250ms to 0ms relative to instructional cue). In this way the MOR for each channel was compared between tap stimuli across three scenarios:

CHAPTER 2. MATERIALS AND METHODOLOGY

Matched force where we compared the MOR between the active and no movement trials that received a 2N reference tap. This allowed a direct comparison between the MOR of trials that received the same absolute force value but whose forces were either self- or externally generated, and thus perceived as different.

Matched perception where we compared the MOR between the active reference tap (i.e., 2N) and the comparison tap that had a value similar to the point of subjective equivalence (PSE). In other words, we compared the MOR of trials that received different absolute force values but were perceived as being similar.

All comparison forces where we calculated the MOR for all the comparison force values in both the active and the no-movement condition. This was done to compare the S1 neural response to the different force intensities.

Note that for the matched-force and the matched-perception comparison scenario, the channels that were flagged as being significantly modulated (marked as being “active”) were based on the 2N active reference tap stimulus whereas for the no movement forces, the channels that were flagged as being significantly modulated (marked as being “active”) were based

on the highest force comparison tap (3N).

2.4.3 Quantifying Somatosensory Attenuation

The participants' responses for both the active and the no movement condition, were independently fitted with a standard logistic function, using equation 2.1

$$F(x; \alpha, \beta) = 1/(1 + \exp(-\beta * (x - \alpha))) \quad (2.1)$$

Where parameter α corresponds to the threshold: $F(x = \alpha, \alpha, \beta,) = 0.5$; parameter β determines the slope of the psychometric function; and x correspond to the signal. We then extracted the point of subjective equality (PSE) from each fitted curve by obtaining the intensity at which the reference tap felt as strong as the comparison tap ($p = 0.5$). PSE represents the intensity at which the reference tap felt as strong as the comparison tap and became our main variable of interest. Using the PSE of each condition, we defined SMA as the difference in PSE between the active (PSE_a) and no movement (PSE_p) conditions (equation 2.2)

$$SMA = PSE_a - PSE_p \quad (2.2)$$

2.5 Statistical Analysis

2.5.1 Calculating difference in MOR across condition

We compared the MOR across three comparison scenarios: matched-force (i.e. 2N active reference vs 2N no movement reference), matched-perception (i.e. 2N active reference vs no movement PSE force, the active and no movement force values for which the participant perceived them as being the same), and all no movement forces. For the matched-force comparison scenario, we used a paired t-test for channels with a normal distribution, otherwise a two-sided Wilcoxon signed-rank test. For the matched-perception scenario, we used a unpaired t-test for channels with a normal distribution, otherwise a two-sided Wilcoxon signed-rank test. For the two scenarios, this was performed at both the individual channels to show which channels showed significant changes between the scenario comparisons as well as a calculated average across all active channels. For the no movement forces, a one-way ANOVA with follow-up post hoc analyses where appropriate was used. Further, we used a linear regression fit in order to look at the relation between the no movement comparison forces and the average MOR response to these force values.

CHAPTER 2. MATERIALS AND METHODOLOGY

In addition, we compared the change in MOR for the two comparison scenarios -matched-force and matched-perception to look for statistically significant differences in the average MOR between conditions. In both cases, we used a two-sided statistical test (for channels with a normal distribution, a paired t-test, otherwise a two-sided Wilcoxon signed-rank test).

2.5.2 Calculating difference in the neural firing rate between Baseline 1(B1) and Baseline (B2)

For comparing the difference in the neural firing rate between B1 and B2 for Pedestal A and B combined for all the trials in the active movement condition, we used a paired t-test to compare the average neural firing rate in the two baselines for all the channels .

All data are given as means \pm SEM. Effects were considered significant if $p < 0.05$.

Chapter 3

Results

3.1 Comparison of behavioral perception of SMA in SCI participant and healthy controls

We used a psychometric curve to quantify SMA behaviorally. As shown in Figure 3.1A, in our SCI participant, we see a perceptual amplification of tap that is generated by the voluntary movement of his hand. Here, the PSE for the active movement was 2.11N, meaning that the 2N self-generated tap is perceived to be equivalent to 2.11N externally generated tap. In the no movement condition, the PSE was 1.99N. Therefore, we quantify the change in PSE as +0.12 N amplification in our SCI participant. In contrast, as shown in Figure

3.1B, in the healthy controls the average PSE for the active movement was 1.747N, meaning that the 2N self-generated tap is perceived to be equivalent to 1.747N externally generated tap. On the other hand the average PSE for the no movement condition is 1.864N. Therefore, we quantify the change in PSE as -0.117N attenuation in our healthy controls.

3.2 Matched-force comparison: Comparison of contralateral S1 MUA in response to 2N active reference tap and 2N no movement reference tap

Figure 3.2 shows that the neural response in contralateral S1 for the self-generated reference tap is greater than the S1 neural response for the externally generated reference tap of the same force intensity (i.e., 2N). Several sensory channels in the contralateral hemisphere show a significant difference in MOR between the self-generated 2N active reference tap and the externally generated 2N no movement reference tap (Figure 3.2A) even though they are of the same force-intensity. As shown in Figure 3.2B, the S1 neural response

CHAPTER 3. RESULTS

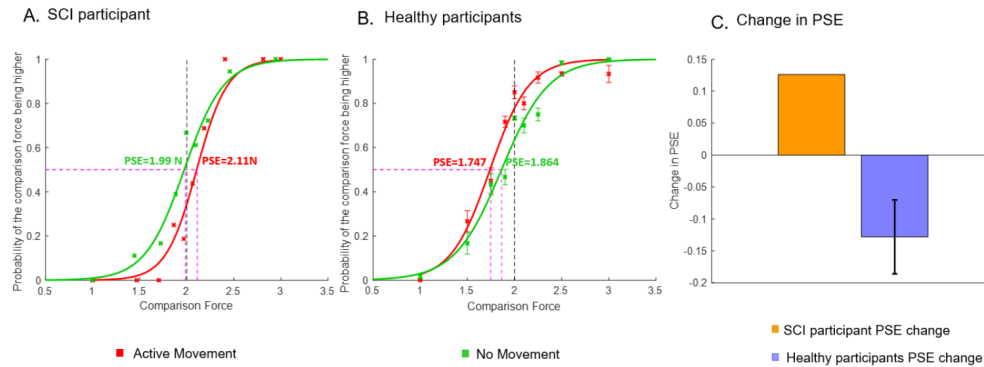


Figure 3.1: Behavioral response for SMA in healthy participants (n=3) and SCI participant: A) The psychometric curve for the SCI participant. The psychometric curve in the active movement condition shifts towards the right indicating a perceptual amplification of self-generated tap when compared to an externally generated tap of the same force intensity of 2N in SCI participant. The x axis denotes the comparison force values and the y-axis denotes the probability that the comparison force is higher than the reference force. Green line represents the no-movement condition, and the red line represents the active movement condition. B) Psychometric curve for healthy participants. The psychometric curve in the active movement condition shifts towards the left indicating a perceptual attenuation of self-generated tap when compared to an externally generated tap of the same force intensity of 2N in healthy participants. The x axis denotes the comparison force values and the y-axis denotes the probability that the comparison force is higher than the reference force. Green line represents the no-movement condition, and the red line represents the active movement condition. C) Bar graph showing the change in PSE between the active movement and no movement condition. SCI participant PSE for active movement condition is 2.11N and the PSE for no movement condition is 1.99N (SMA=+0.12N (yellow)). For healthy participants, average PSE for active movement condition is 1.747 and PSE for no movement PSE condition is 1.864 (SMA=-0.117(light purple)). y-axis denotes the change in PSE.

CHAPTER 3. RESULTS

for an example sensory channel (highlighted in pink in Figure 3.2A show that the neural response to the tap that is generated by the voluntary movement of the participant's hand (active movement) was significantly higher than the S1 neural response for the externally generated tap (no movement condition) of the same force intensity of 2N. The average MOR across all active channels for the self-generated tap was significantly larger compared to the externally generated tap of the same force intensity (***) $p < 0.001$). This is in accordance with what was observed behaviorally in the psychometric curve (Figure 3.1A) where the active reference tap of 2N was perceived to be of a higher intensity and had a higher PSE in comparison to the no movement reference tap of 2N. Therefore, our SCI participant showed an amplification of self-generated tap when compared to an externally generated tap of the same force-intensity both perceptually and neurophysiologically in his multi-unit contralateral S1 activity.

CHAPTER 3. RESULTS

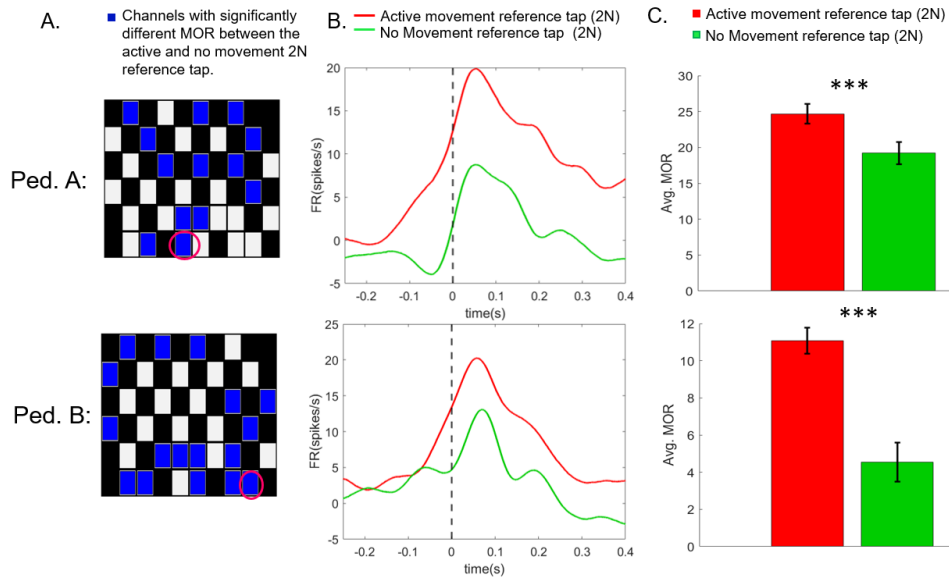


Figure 3.2: Matched-force comparison- S1 response for active movement reference tap and no movement reference tap at force intensity of 2N: A) Represents the sensory MEAs in the participants contralateral hemisphere (top from Pedestal A and bottom from Pedestal B). Channels that are highlighted in blue represent a significant difference in the magnitude of response (MOR) between the active movement and no movement reference tap of 2N. An example PETH for the channels is marked by a pink circle and expanded upon in 3.2B. B) Example PETH plots of two channels that show significant difference in the MOR in Pedestal A (top) and B (bottom) show the neural response in S1 to the active movement reference tap at 2N (in red) and the no movement reference tap at 2N (in green). The dashed black line represents the time of the tap stimulus onset (reference tap). The x-axis denotes the time (in s) and y-axis denotes the firing rate in spikes/s. C) The bar graph shows the average MOR (mean \pm SEM) for the active movement reference tap of 2N (red) and the no movement reference tap of 2N (green). The average MORs for the active movement was significantly higher than the no movement condition for both pedestal A and B (*** $p < 0.001$). y-axis denotes the average MOR in spikes/s.

3.3 Matched-perception comparison: Comparison of contralateral S1 MUA for self-generated tap of 2N and externally generated tap at the PSE

Figure 3.3 shows that the neural response in contralateral S1 for the 2N self-generated reference tap is similar to the S1 neural response for the externally generated comparison tap at the point of subjective equality (2.1N). No sensory channels in Pedestal A show a significant difference in MOR between the self-generated 2N active reference tap and the externally generated 2.1N comparison tap and only one sensory channel in Pedestal B show a significant difference in MOR between the self-generated 2N active reference tap and the externally generated 2.1N comparison tap (Figure 3.3A) even though they are of different absolute force intensities. As shown in Figure 3.3B, the S1 neural response for an example sensory channel (highlighted in pink in Figure 3.3A) show that the neural response to the tap that is generated by the voluntary movement of the participant's hand (active movement) was similar to the S1 neural response for comparison tap of 2.1N. The average MOR across all active channels for the self-generated tap was not significantly different compared to

CHAPTER 3. RESULTS

the externally generated tap of 2.1N. ($p=0.6866$) in pedestal A and was significantly different in pedestal B ($p=0.03$) (Figure 3.3C) . This is in accordance with what was observed behaviorally in the psychometric curve (Figure 3.1A) where the active reference tap of 2N was perceived to be equal to an externally generated tap of 2.11N. Therefore we see a correlation between the behavioral perception and the neural response in S1 to these two forces.

3.4 Change in the MOR for matched-force and matched-perception: Comparison between Δ MOR for matched-force and matched-perception

We subsequently compared the change in the average MOR between the two matched-perception and compared it to the change in average MOR between the two matched-force conditions (Figure 3.4). We found that the magnitude of change was significantly higher for the matched-forces condition than the matched-perception condition for both Pedestal A ($p<0.001$) and pedestal B ($p<0.001$).

CHAPTER 3. RESULTS

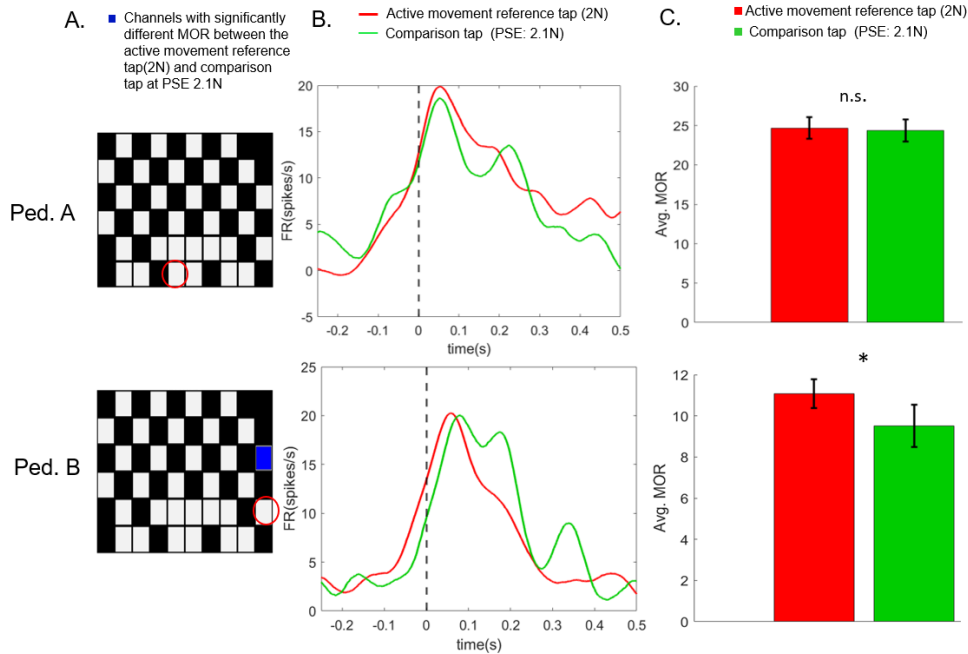


Figure 3.3: Matched-perception comparison: S1 multi-unit neural response for 2N active reference tap and comparison tap at PSE (2.1 N comparison tap): A) Represents the sensory MEAs for Pedestal A (top) and B (bottom) sensory channels of the contralateral hemisphere. No channels in Ped A showed a significant difference in the MOR between the two matched-perception conditions and only 1 channel in pedestal B (highlighted by blue) showed a significant difference in the MOR between the two conditions ($p < 0.05$). B) Example PETH plots of channels highlighted by pink circle in figure 3.3A. The peak S1 response to the two matched-perception forces appear similar. The dashed black line represents the time of the tap stimulus onset (reference tap/ comparison tap). The x-axis denotes the time (in s) and y-axis denotes the firing rate in spikes/s. C) The bar graph shows the average MOR (mean \pm SEM) for the active movement reference tap (red) at 2N and the 2.1N PSE comparison tap (green). There was no significant difference in Pedestal A between the active movement reference tap of 2N (red) and the PSE comparison tap at 2.1N (green), ($p = 0.6866$), however, there was in Pedestal B, with 2N reference tap average MOR (red) showing a significant increase compared to the 2.1N PSE (green) ($p = 0.03$). y-axis denotes the average MOR in spikes/s. (* $p < 0.05$ denoting significantly different, n.s. denotes not significantly different)

CHAPTER 3. RESULTS

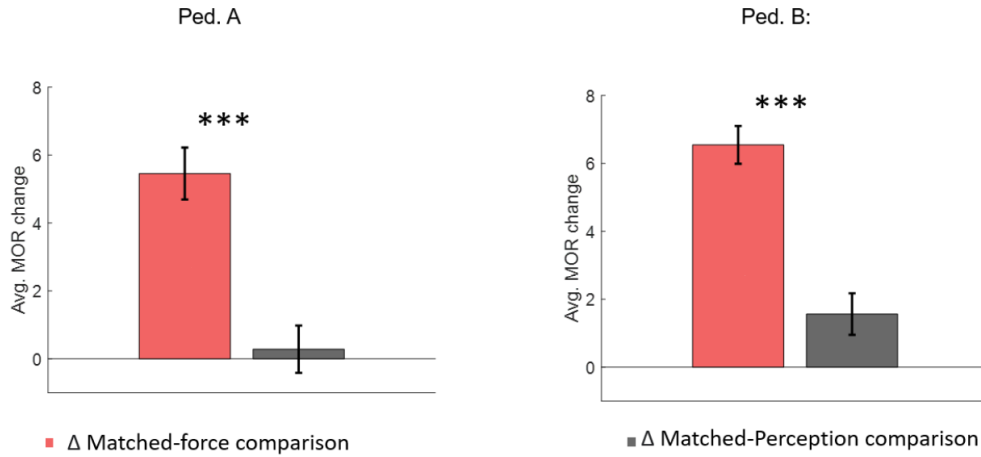


Figure 3.4: Change in average MOR(Δ) between the matched-force and the matched-perception conditions: A) Shows the change in average MOR between the matched-force condition (2N active ref. Vs 2N no movement ref.) and the matched-perception condition (2N active ref. Vs 2.1N (PSE) comparison) in pedestal A. The change in MOR was significantly greater in the matched-force condition as compared to matched-perception condition (***) $p < 0.001$. B) Shows the change in average MOR between the matched-force condition (2N active ref. Vs 2N no movement ref.) and the matched-perception condition (2N active ref. Vs 2.1N (PSE) comparison) in pedestal B. Similarly, there was a significantly greater change in MOR for the matched-force as compared to matched-perception condition. (***) $p < 0.001$. y-axis denotes the average MOR in spikes/s.

The change in the average MOR (Δ) for the matched-force comparison is more than the matched-perception condition. Which implies that the perception of the self-generated tap is correlated to the S1 multi-unit neural response to that tap. That is when the participant perceives the self and externally generated tap of the same force intensity to be different, the S1 multi-unit response shown by the average MOR to the two 2N tap which is self-generated

CHAPTER 3. RESULTS

and externally generated is also different. (Higher change in MOR). But at the point of subjective equality (PSE), when the participant perceives the self and externally generated tap to be the same, the S1 multi-unit response to the two taps is more similar - as shown by lower changes in average MOR.

3.5 Average MOR response for all no-movement comparison force intensities

Figure 3.5 shows the average contralateral S1 MOR response to all the no-movement force intensities.

Using a one-way ANOVA comparing the MOR across different force intensities, we found a significant effect for force for both Pedestal A and B, showing that the S1 multi-unit neural response varies depending on the force intensity of the tap provided to the participant's index finger in both the pedestals. For pedestal A ($F=8.28$, $p<.01$), the MOR for 3N is significantly higher than 1N ($p<0.001$), 1.5N ($p<0.001$), 1.75N ($p<0.001$), 1.9N ($p<0.01$), 2N ($p<0.001$), 2.25N ($p<0.01$) and 2.5N ($p<0.01$). The MOR for 2.1 N is significantly higher than 1N($p<0.001$), 1.5N ($p<0.01$), 1.75N ($p<0.05$) and 2N($p<0.05$). For pedestal

CHAPTER 3. RESULTS

B ($F=7.69$, $p<0.01$), the MOR for 3N is significantly higher than 1N ($p<0.001$), 1.5N ($p<0.001$), 1.75N ($p<0.001$), 1.9N ($p<0.001$), 2N ($p<0.001$), 2.25N ($p<0.001$) and 2.5N ($p<0.001$). The MOR for 2.1 N is significantly higher than 1.5N ($p<0.05$), 1.75N ($p<0.01$), and 2N ($p<0.001$).

We used a linear regression fit to compare the relation between the comparison forces and the average MOR response to these forces. For pedestal A, we got a R-squared value of 0.682 and $p<0.001$. For Pedestal B, we got a R-squared of 0.399 and p value of 0.068. This implies that there is a linear relation between comparison force value and MOR response in pedestal A and a general increase in MOR response with comparison force values in pedestal B.

3.6 Preparatory neural activity: Comparison between average neural firing rate in baseline 1(B1) and baseline 2 (B2)

No significant difference was observed between the average firing rate in B1 and B2. ($p=0.85$) as shown in Figure 3.6

CHAPTER 3. RESULTS

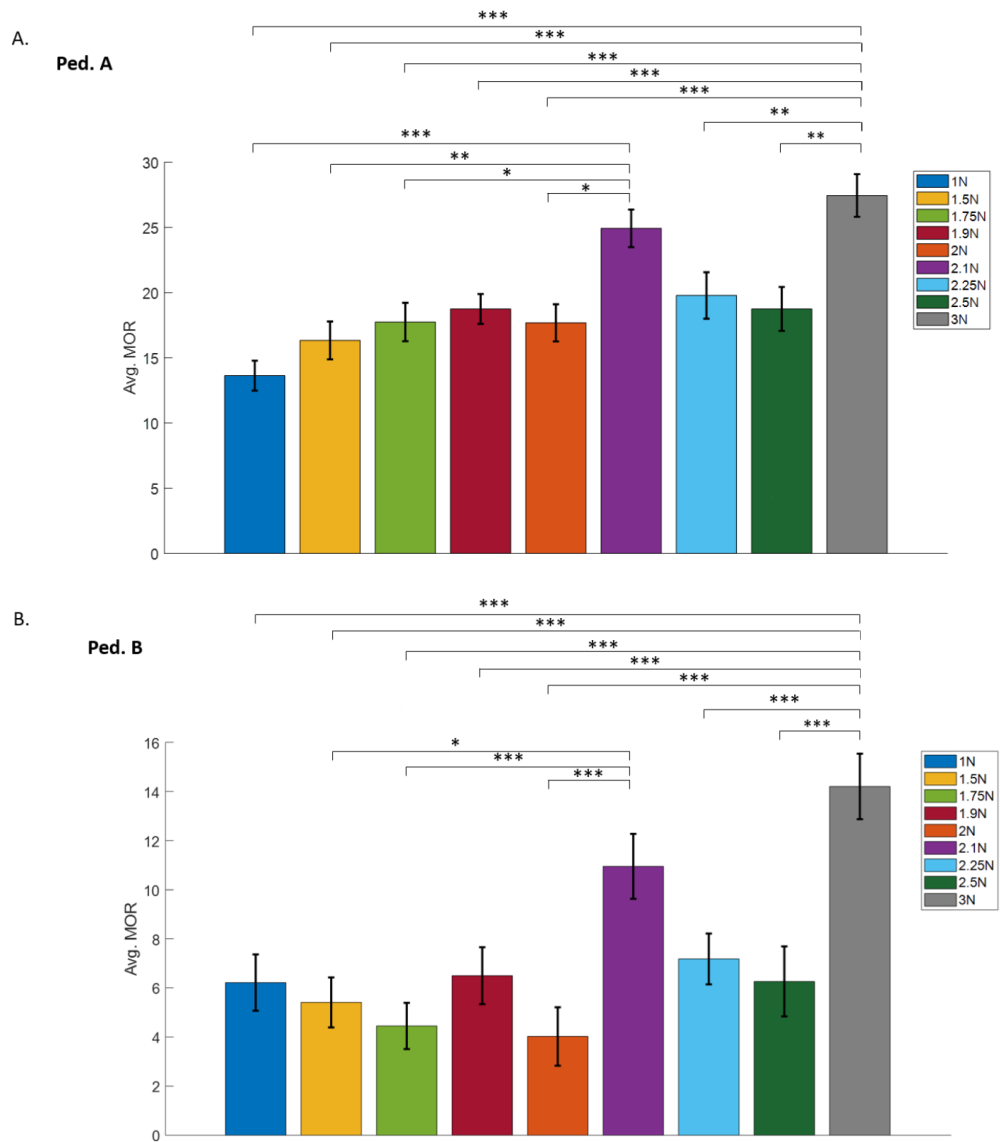


Figure 3.5: Average contralateral S1 MOR response for all comparison forces: A) Bar graph represents the Average MOR (+/-SEM) for all the different comparison force intensities (1N, 1.5N, 1.75N, 1.9N, 2N, 2.1N, 2.25N, 2.5N, 3N) in pedestal A (* $p < 0.05$, ** $p < 0.01$, *** $p < 0.001$). y-axis denotes the average MOR in spikes/s. B) Bar graph represents the Average MOR +/-SEM for all the different comparison force intensities (1N, 1.5N, 1.75N, 1.9N, 2N, 2.1N, 2.25N, 2.5N, 3N) in pedestal B (* $p < 0.05$, ** $p < 0.01$, *** $p < 0.001$). y-axis denotes the average MOR in spikes/s.

CHAPTER 3. RESULTS

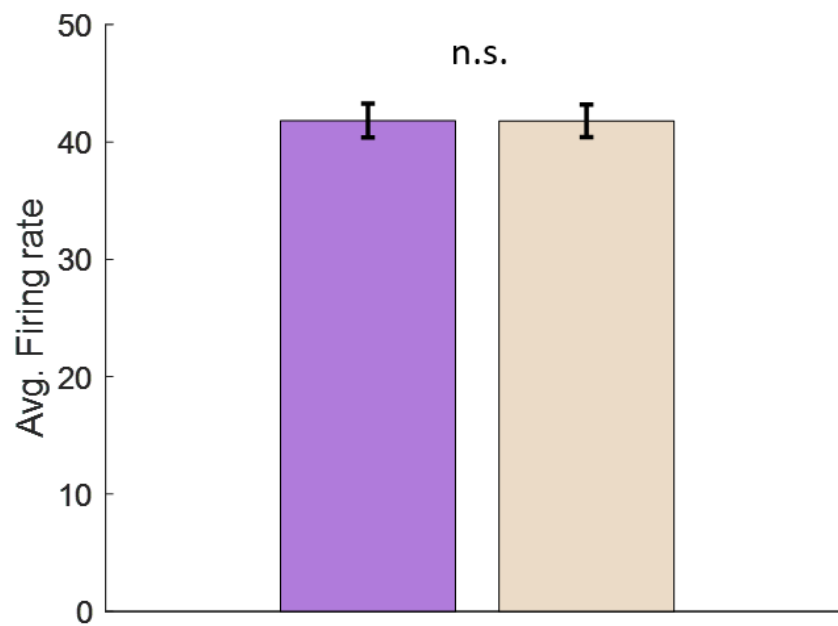


Figure 3.6: Comparison of the average firing rate between B1 and B2: Bar graph represents the average firing rate (\pm -SEM) in B1 (purple) and the average firing rate (\pm -SEM) in B2 (beige) for pedestal A and B combined. The y-axis denotes the average firing rate in spikes/s. (n.s (not significant))

Chapter 4

Observation and Conclusion

4.1 Observation

In this study, we aimed to understand the S1 neurophysiological correlate of SMA and how it relates with perceptual behavior. The results of our study demonstrate that the SCI participant in our study showed an amplification of his self-generated tap when compared to an externally generated tap of the same force intensity both perceptually and neurophysiologically in S1. Behaviorally, our SCI participant perceived his self-generated tap to be of a higher intensity than the externally generated tap of the same force intensity. Similarly, the multi-unit neural activity in S1 was greater for his self-generated tap when compared to an externally generated tap of the same force intensity. Furthermore, we showed that when the participant perceived the self and ex-

CHAPTER 4. OBSERVATION AND CONCLUSION

ternally generated taps to be of the same intensity, the S1 MUA was similar for the two forces. On the other hand, our healthy controls showed a perceptual attenuation of their self-generated tap when compared to an externally generated tap of the same force intensity.

The attenuation of self-generated forces that was seen in healthy controls is consistent with previous work^{1;3;11}. However, the amplification of self-generated forces in our SCI participant was contrary to our predictions. No study to date has looked at sensorimotor attenuation in SCI participants and our understanding of the interaction between the sensory and motor systems in SCI patients that play a pivotal role in the underlying mechanisms of SMA is limited. There are three possible, though non-mutually exclusive, reasons for the observed amplification in our participant: attention to self-stimuli, limited agency, and cortical reorganization.

Attenuation of the sensory consequences of self-generated movements in healthy controls is an important mechanism to heighten salience of stimuli arising from the environment and to reduce the cognitive load arising from the sensory consequences of self-generated stimuli². Since SCI patients must pay more attention to their own bodily movements to improve their motor abilities^{30;31}, it is possible that their nervous system amplifies the perceptual con-

CHAPTER 4. OBSERVATION AND CONCLUSION

sequences of their own actions to highlight self-generated actions rather than the environment. Indeed, the heightened attention to bodily sensations has shown to cause somatosensory amplification in patients with somatoform disorders which are a group of psychological conditions where patients experience bodily physical sensations and pain without any underlying medical diagnosis^{32;33}. It is possible, therefore, that patients with SCI amplify, rather than attenuate, the sensory consequence of their own movements to improve their motor control.

Agency and body ownership are key factors contributing to somatosensory attenuation^{3;11;34}. SCI patients, however, have disownership and feelings of detachment from their own body^{35;36}. SCI patients commonly experience involuntary movements such as tremor, increased hyperreflexia, clonus, as well as muscle spasms and spasticity³⁷. In addition, they commonly experience phantom sensations (i.e., phantom limb and phantom pain) and neuropathic pain below the site of their spinal cord injury, where they have a complete loss of sensory input^{38;39}. It is possible, therefore, that the observed somatosensory amplification indicates lower agency and body ownership in SCI. In line with this idea, other neurodegenerative disorders that induce involuntary movements and loss of motor control, such as multiple sclerosis (MS)^{13;15} and Parkinson's disease (PD)¹⁴, do not show somatosensory attenuation of self-generated move-

CHAPTER 4. OBSERVATION AND CONCLUSION

ments. Thus, the lack of agency over voluntary movements observed in our SCI participant could cause an amplification instead of an attenuation of self-generated stimuli.

The functional connectivity between S1 and other brain regions plays an important role in SMA¹¹. The shift in cortical activation patterns and neural pathways following SCI could alter the underlying mechanisms of SMA in SCI patients. Cortical reorganization and neural plasticity of neural networks is commonly observed following the spinal cord injury in patients in order to compensate for the lost sensory and motor functions⁴⁰⁻⁴². This leads to the development of new neural networks and pathways in these patients. For example, there is a posterior shift in the neural activity in the cortex following SCI. Green et al. (1999)⁴³ have proposed that an increased loss of axons in M1 following SCI may lead to surviving axons from S1 contributing to the damaged corticospinal tract, thus leading to a greater activity in S1. Furthermore, SCI has shown to cause a distortion in the input/output signal transmission and reduction in the functional connectivity between M1 and S1⁴¹. All these changes in the sensorimotor cortex can alter the mechanisms of SMA that are found to occur in healthy individuals.

Importantly, in this study we found that the perceptual intensity of the

CHAPTER 4. OBSERVATION AND CONCLUSION

tap stimuli correlates with the magnitude of the multi-unit neural response in S1. In our study, we observed that when the participant perceived his self-generated force of 2N to be higher than an externally generated force of 2N, the S1 neural response to the self-generated tap of 2N was significantly higher than the neural response to the externally generated tap of 2N. Similarly, when two different force intensities were perceived to be similar (i.e., at the PSE), the S1 multi-unit neural response to the two forces was also similar. This is consistent with what has been observed previously in the literature. Kiteni et. al showed that behavioral perception of stimuli correlates to the blood oxygen level-dependent (BOLD) response in the right and left supramarginal gyri. That is, when the touch is perceived to be of a lower intensity, the blood oxygen level-dependent (BOLD) response is also lower, and the BOLD response is higher when the touch is perceived to be of a higher intensity. Similarly, sensory evoked potentials in S1 of healthy participants are smaller for self-generated forces than an externally generated force of the same intensity^{44;45}. Similar results were also shown in healthy NHP model by Jiang et al. where they showed an attenuation of S1 multi-unit activity following ICMS on M1 prior to movement onset²⁹.

Our study shows interesting results about the perception and S1 multi-unit response to self-generated and externally generated stimuli in SCI patients

CHAPTER 4. OBSERVATION AND CONCLUSION

and how they are different from healthy controls. The understanding of sensory response to different types of stimuli following spinal cord injury would help in the development of new rehabilitation plans for not only patients with SCI but also for patients with other neurological disorders and stroke. Loss of agency over voluntary movements in patients with neurological diseases is found to increase with the progression of the disease^{46;47}. Therefore, SMA score could be used clinically as a tool to quantify the progression of the disease or to measure improvements in motor control in these patients following rehabilitation. Further, it can also be used in the development of better prosthesis and BMI-controlled devices that could be more embodied by these patients.

4.2 Limitations and Next Steps

Our study only looks at the data from a single SCI participant. A larger sample size is important to strongly conclude amplification of self-generated forces in comparison to externally generated forces in SCI patients. The extent and the degree of the spinal cord injury might vary the results that we see in this study. The sample size of healthy controls in our study was small($n=3$). The next steps would be to conduct the study on a larger healthy controls sample. We also plan on studying SMA behaviorally on other SCI participants.

CHAPTER 4. OBSERVATION AND CONCLUSION

In our current analysis we did not see a significant difference in the instructional and preparatory baselines. As a next step, we will look specifically at the channels with large modulations for the self-generated tap and see if we can find any difference in the instructional and preparatory baseline firing rate. We will also look for the presence of efference copy in S1 after movement onset for the self-generated movement condition.

4.3 Conclusion

Our current study compares the behavioral and the S1 multi-unit neurophysiological correlation of SMA in a chronically implanted SCI participant. The results of our study suggest that an amplification of self-generated forces compared to externally generated force of the same intensity (somatosensory amplification) is seen in our SCI participant and that there is a similar relationship between the change in multi-unit neural activity to a force in S1 and the behavioral perception of that force. These findings of our study would help in better understanding the S1 somatosensory neurophysiology in general and particularly in SCI patients and would help in the development of more effective rehabilitation plans for patients affected by spinal cord injury, stroke, and other neurodegenerative disorders.

Bibliography

- [1] K. Kilteni, P. Engeler, and H. H. Ehrsson, “Efference Copy Is Necessary for the Attenuation of Self-Generated Touch,” *iScience*, vol. 23, no. 2, p. 100843, 2020. [Online]. Available: <https://www.sciencedirect.com/science/article/pii/S2589004220300262>
- [2] S. J. Blakemore, D. Wolpert, and C. Frith, “Why can’t you tickle yourself?” *Neuroreport*, vol. 11, no. 11, pp. R11–16, Aug. 2000.
- [3] S. S. Shergill, “Two Eyes for an Eye: The Neuroscience of Force Escalation,” *Science*, vol. 301, no. 5630, pp. 187–187, Jul. 2003. [Online]. Available: <https://www.sciencemag.org/lookup/doi/10.1126/science.1085327>
- [4] P. M. Bays, D. M. Wolpert, and J. R. Flanagan, “Perception of the Consequences of Self-Action Is Temporally Tuned and Event Driven,” *Current Biology*, vol. 15, no. 12, pp. 1125–1128, Jun. 2005. [Online]. Available: <https://linkinghub.elsevier.com/retrieve/pii/S0960982205005117>

BIBLIOGRAPHY

- [5] S. J. Blakemore, D. M. Wolpert, and C. D. Frith, “Central cancellation of self-produced tickle sensation,” *Nat Neurosci*, vol. 1, no. 7, pp. 635–640, Nov. 1998.
- [6] B. P. Rummell, J. L. Klee, and T. Sigurdsson, “Attenuation of Responses to Self-Generated Sounds in Auditory Cortical Neurons,” *J Neurosci*, vol. 36, no. 47, pp. 12 010–12 026, Nov. 2016.
- [7] M. G. Phillips, S. C. Lenzi, and J. P. Geerts, “Cortical Predictive Mechanisms of Auditory Response Attenuation to Self-Generated Sounds,” *J Neurosci*, vol. 37, no. 22, pp. 5393–5394, May 2017. [Online]. Available: <https://www.ncbi.nlm.nih.gov/pmc/articles/PMC5452336/>
- [8] N. G. Mifsud, T. Beesley, T. L. Watson, R. B. Elijah, T. S. Sharp, and T. J. Whitford, “Attenuation of visual evoked responses to hand and saccade-initiated flashes,” *Cognition*, vol. 179, pp. 14–22, Oct. 2018. [Online]. Available: <https://www.sciencedirect.com/science/article/pii/S0010027718301574>
- [9] K. A. Schwarz, R. Pfister, M. Kluge, L. Weller, and W. Kunde, “Do we see it or not? Sensory attenuation in the visual domain,” *Journal of Experimental Psychology: General*, vol. 147, no. 3, pp. 418–430, 2018, place: US Publisher: American Psychological Association.
- [10] P. Bays, J. Flanagan, and D. Wolpert, “Attenuation of Self-Generated Tac-

BIBLIOGRAPHY

- tile Sensations Is Predictive, not Postdictive,” *PLoS biology*, vol. 4, p. e28, Mar. 2006.
- [11] K. Kilteni and H. H. Ehrsson, “Functional Connectivity between the Cerebellum and Somatosensory Areas Implements the Attenuation of Self-Generated Touch,” *J Neurosci*, vol. 40, no. 4, pp. 894–906, Jan. 2020.
- [12] K. Kilteni, C. Houborg, and H. H. Ehrsson, “Rapid learning and unlearning of predicted sensory delays in self-generated touch,” *Elife*, vol. 8, Nov. 2019.
- [13] D. J. Arpin, J. E. Gehringer, T. W. Wilson, and M. J. Kurz, “A reduced somatosensory gating response in individuals with multiple sclerosis is related to walking impairment,” *APSselect*, vol. 4, no. 9, pp. 2052–2058, Jul. 2017, publisher: American Physiological Society. [Online]. Available: <https://journals.physiology.org/doi/full/10.1152/jn.00260.2017%40apsselect.2017.4.issue-9>
- [14] N. Wolpe, J. Zhang, C. Nombela, J. N. Ingram, D. M. Wolpert, and J. B. Rowe, “Sensory attenuation in Parkinson’s disease is related to disease severity and dopamine dose,” *Scientific Reports*, vol. 8, no. 1, p. 15643, Oct. 2018, number: 1 Publisher: Nature Publishing Group. [Online]. Available: <https://www.nature.com/articles/s41598-018-33678-3>
- [15] D. J. Arpin, J. E. Gehringer, T. W. Wilson, and M. J. Kurz, “Movement-

BIBLIOGRAPHY

- Related Somatosensory Activity Is Altered in Patients with Multiple Sclerosis,” *Brain Topogr*, vol. 31, no. 4, pp. 700–707, Jul. 2018.
- [16] S. S. Shergill, T. P. White, D. W. Joyce, P. M. Bays, D. M. Wolpert, and C. D. Frith, “Functional Magnetic Resonance Imaging of Impaired Sensory Prediction in Schizophrenia,” *JAMA Psychiatry*, vol. 71, no. 1, p. 28, Jan. 2014. [Online]. Available: <http://archpsyc.jamanetwork.com/article.aspx?doi=10.1001/jamapsychiatry.2013.2974>
- [17] M. Kawato, “Internal models for motor control and trajectory planning,” *Curr Opin Neurobiol*, vol. 9, no. 6, pp. 718–727, Dec. 1999.
- [18] D. Franklin and D. Wolpert, “Computational Mechanisms of Sensorimotor Control,” *Neuron*, vol. 72, no. 3, pp. 425–442, Nov. 2011. [Online]. Available: <https://linkinghub.elsevier.com/retrieve/pii/S0896627311008919>
- [19] P. R. Davidson and D. M. Wolpert, “Widespread access to predictive models in the motor system: a short review,” *Journal of neural engineering*, p. 7, 2005.
- [20] D. M. Wolpert, R. C. Miall, and M. Kawato, “Internal models in the cerebellum,” *Trends Cogn Sci*, vol. 2, no. 9, pp. 338–347, Sep. 1998.
- [21] R. Shadmehr and J. W. Krakauer, “A computational neuroanatomy for

BIBLIOGRAPHY

- motor control,” *Exp Brain Res*, vol. 185, no. 3, pp. 359–381, Mar. 2008.
[Online]. Available: <https://doi.org/10.1007/s00221-008-1280-5>
- [22] R. Shadmehr, M. A. Smith, and J. W. Krakauer, “Error correction, sensory prediction, and adaptation in motor control,” *Annu Rev Neurosci*, vol. 33, pp. 89–108, 2010.
- [23] A. S. Therrien and A. J. Bastian, “The cerebellum as a movement sensor,” *Neurosci Lett*, vol. 688, pp. 37–40, Jan. 2019.
- [24] A. Macerollo, J.-C. Chen, I. Pareés, P. Kassavetis, J. M. Kilner, and M. J. Edwards, “Sensory Attenuation Assessed by Sensory Evoked Potentials in Functional Movement Disorders,” *PLoS One*, vol. 10, no. 6, p. e0129507, 2015.
- [25] M. Dogge, D. Hofman, R. Custers, and H. Aarts, “Exploring the role of motor and non-motor predictive mechanisms in sensory attenuation: Perceptual and neurophysiological findings,” *Neuropsychologia*, vol. 124, pp. 216–225, Feb. 2019. [Online]. Available: <https://www.sciencedirect.com/science/article/pii/S0028393218304160>
- [26] P. Hazemann, G. Audin, and F. Lille, “Effect of voluntary self-paced movements upon auditory and somatosensory evoked potentials in man,” *Electroencephalography and Clinical Neurophysiology*, vol. 39, no. 3, pp.

BIBLIOGRAPHY

- 247–254, Sep. 1975. [Online]. Available: <https://www.sciencedirect.com/science/article/pii/0013469475901467>
- [27] R. Boehme, S. Hauser, G. J. Gerling, M. Heilig, and H. Olausson, “Distinction of self-produced touch and social touch at cortical and spinal cord levels,” *PNAS*, vol. 116, no. 6, pp. 2290–2299, Feb. 2019, publisher: National Academy of Sciences Section: PNAS Plus. [Online]. Available: <https://www.pnas.org/content/116/6/2290>
- [28] S. S. Shergill, T. P. White, D. W. Joyce, P. M. Bays, D. M. Wolpert, and C. D. Frith, “Modulation of somatosensory processing by action,” *NeuroImage*, vol. 70, pp. 356–362, Apr. 2013. [Online]. Available: <https://linkinghub.elsevier.com/retrieve/pii/S1053811912012293>
- [29] W. Jiang, C. E. Chapman, and Y. Lamarre, “Modulation of somatosensory evoked responses in the primary somatosensory cortex produced by intracortical microstimulation of the motor cortex in the monkey,” *Exp Brain Res*, vol. 80, no. 2, pp. 333–344, 1990.
- [30] M. Dimitriou, “Enhanced Muscle Afferent Signals during Motor Learning in Humans,” *Current Biology*, vol. 26, no. 8, pp. 1062–1068, Apr. 2016. [Online]. Available: <https://www.sciencedirect.com/science/article/pii/S0960982216300835>
- [31] A. Takeoka, I. Vollenweider, G. Courtine, and S. Arber, “Muscle Spindle

BIBLIOGRAPHY

- Feedback Directs Locomotor Recovery and Circuit Reorganization after Spinal Cord Injury,” *Cell*, vol. 159, no. 7, pp. 1626–1639, Dec. 2014, publisher: Elsevier. [Online]. Available: [https://www.cell.com/cell/abstract/S0092-8674\(14\)01450-0](https://www.cell.com/cell/abstract/S0092-8674(14)01450-0)
- [32] M. Nakao and A. J. Barsky, “Clinical application of somatosensory amplification in psychosomatic medicine,” *Biopsychosoc Med*, vol. 1, p. 17, Oct. 2007.
- [33] D. L. Perez, A. J. Barsky, D. R. Vago, G. Baslet, and D. A. Silbersweig, “A Neural Circuit Framework for Somatosensory Amplification in Somatoform Disorders,” *JNP*, vol. 27, no. 1, pp. e40–e50, Nov. 2014, publisher: American Psychiatric Publishing. [Online]. Available: <https://neuro.psychiatryonline.org/doi/full/10.1176/appi.neuropsych.13070170>
- [34] K. Kilteni and H. H. Ehrsson, “Body ownership determines the attenuation of self-generated tactile sensations,” *PNAS*, vol. 114, no. 31, pp. 8426–8431, Aug. 2017, publisher: National Academy of Sciences Section: Biological Sciences. [Online]. Available: <https://www.pnas.org/content/114/31/8426>
- [35] B. Lenggenhager, M. Pazzaglia, G. Scivoletto, M. Molinari, and S. M. Aglioti, “The Sense of the Body in Individuals with Spinal Cord Injury,” *PLOS ONE*, vol. 7, no. 11, p. e50757, Nov. 2012,

BIBLIOGRAPHY

- publisher: Public Library of Science. [Online]. Available: <https://journals.plos.org/plosone/article?id=10.1371/journal.pone.0050757>
- [36] T. E. Ham, V. Bonnelle, P. Hellyer, S. Jilka, I. H. Robertson, R. Leech, and D. J. Sharp, “The neural basis of impaired self-awareness after traumatic brain injury,” *Brain*, vol. 137, no. 2, pp. 586–597, Feb. 2014. [Online]. Available: <https://doi.org/10.1093/brain/awt350>
- [37] N. Sezer, S. Akkuş, and F. G. Uğurlu, “Chronic complications of spinal cord injury,” *World J Orthop*, vol. 6, no. 1, pp. 24–33, Jan. 2015. [Online]. Available: <https://www.ncbi.nlm.nih.gov/pmc/articles/PMC4303787/>
- [38] “Neuropathic Pain After Spinal Cord Injury: Challenges and Research Perspectives.” [Online]. Available: <https://www.ncbi.nlm.nih.gov/pmc/articles/PMC6095789/>
- [39] J. Y. Choi, H. I. Kim, K. C. Lee, and Z.-A. Han, “Atypical Supernumerary Phantom Limb and Phantom Limb Pain in a Patient With Spinal Cord Injury: Case Report,” *Ann Rehabil Med*, vol. 37, no. 6, pp. 901–906, Dec. 2013. [Online]. Available: <https://www.ncbi.nlm.nih.gov/pmc/articles/PMC3895533/>
- [40] P. Freund, N. Weiskopf, N. S. Ward, C. Hutton, A. Gall, O. Ciccarelli, M. Craggs, K. Friston, and A. J. Thompson, “Disability, atrophy and cortical reorganization following spinal cord injury,” *Brain*,

BIBLIOGRAPHY

- vol. 134, no. 6, pp. 1610–1622, Jun. 2011. [Online]. Available: <https://www.ncbi.nlm.nih.gov/pmc/articles/PMC3102242/>
- [41] A. H. Hawasli, J. Rutlin, J. L. Roland, R. K. Murphy, S.-K. Song, E. C. Leuthardt, J. S. Shimony, and W. Z. Ray, “Spinal Cord Injury Disrupts Resting-State Networks in the Human Brain,” *J Neurotrauma*, vol. 35, no. 6, pp. 864–873, Mar. 2018. [Online]. Available: <https://www.ncbi.nlm.nih.gov/pmc/articles/PMC5863102/>
- [42] K. J. Kokotilo, J. J. Eng, and A. Curt, “Reorganization and Preservation of Motor Control of the Brain in Spinal Cord Injury: A Systematic Review,” *J Neurotrauma*, vol. 26, no. 11, pp. 2113–2126, Nov. 2009. [Online]. Available: <https://www.ncbi.nlm.nih.gov/pmc/articles/PMC3167869/>
- [43] J. B. Green, E. Sora, Y. Bialy, A. Ricamato, and R. W. Thatcher, “Cortical motor reorganization after paraplegia: an EEG study,” *Neurology*, vol. 53, no. 4, pp. 736–743, Sep. 1999.
- [44] H. Kirimoto, A. Asao, H. Tamaki, and H. Onishi, “Non-invasive modulation of somatosensory evoked potentials by the application of static magnetic fields over the primary and supplementary motor cortices,” *Scientific Reports*, vol. 6, no. 1, p. 34509, Oct. 2016, number: 1 Publisher: Nature Publishing Group. [Online]. Available: <https://www.nature.com/articles/srep34509>

BIBLIOGRAPHY

- [45] H. Nakata, K. Inui, T. Wasaka, Y. Nishihira, and R. Kakigi, “Mechanisms of Differences in Gating Effects on Short- and Long-Latency Somatosensory Evoked Potentials Relating to Movement,” *Brain Topogr*, vol. 15, no. 4, pp. 211–222, Jun. 2003. [Online]. Available: <https://doi.org/10.1023/A:1023908707851>
- [46] J. W. Moore and P. C. Fletcher, “Sense of agency in health and disease: A review of cue integration approaches,” *Consciousness and Cognition*, vol. 21, no. 1, pp. 59–68, Mar. 2012. [Online]. Available: <https://www.sciencedirect.com/science/article/pii/S1053810011002005>
- [47] C. D. Frith, S. J. Blakemore, and D. M. Wolpert, “Abnormalities in the awareness and control of action.” *Philos Trans R Soc Lond B Biol Sci*, vol. 355, no. 1404, pp. 1771–1788, Dec. 2000. [Online]. Available: <https://www.ncbi.nlm.nih.gov/pmc/articles/PMC1692910/>

Vita



Teresa George was born on March 6th, 1997 in Kerala, India. She spend her early childhood years in different parts of India before she moved to Dubai, United Arab Emirates at the age of 12. The exposure to science and mathematics she received during her high school days, encouraged her to pursue engineering as a career. She graduated with a undergraduate degree in Electronics and Communication Engineering from Birla Institute of Technology and Sci-

VITA

ence in Dubai. Her motivation to use her skills in engineering to make a direct impact in healthcare and medicine led to her decision to pursue Masters in Biomedical Engineering from Johns Hopkins University.

At Hopkins she worked in the Haptics and Medical Robotics (HAMR) Laboratory under the guidance of Dr. Jeremy Brown on a collaborative project with the Brain, Learning, Animation, and Movement (BLAM) Laboratory, where she worked on improving the hardware of the hand device used to study the hand dexterity and movements in patients recovering from stroke. She worked on the inclusion of vibrotactile haptic feedback to the device to understand how haptics could help in stroke rehabilitation.

In the final year of her masters, she worked under the guidance of Dr. Jeremy Brown and Dr. Gabriela Cantarero in the The Human Brain Physiology and Stimulation Laboratory where she studied the underlying sensorimotor neurophysiology of somatosensory attenuation in a spinal cord injury participant and on understanding the supraspinal underpinnings of fatigue.

In the future, she plans to use the knowledge and skills she learned at Hopkins and through this project to make a wider contribution in the field of neuroscience and in the development of better rehabilitation techniques for patients affected by various neurological disorders.